Evidence for Anomalous Hydration Dynamics near a Model Hydrophobic Peptide†

Daniela Russo,‡,§ Rajesh K. Murarka,‡,§ Greg Hura,|| Elizabeth Verschell,|| John R. D. Copley,⊥ and Teresa Head-Gordon*,‡,||

Department of Bioengineering and Graduate Group in Biophysics, University of California, Berkeley, California 94720, and National Institute of Standards and Technology, Gaithersburg, Maryland 20899-8562

Received: July 15, 2004; In Final Form: October 4, 2004

We present new quasi-elastic neutron scattering experiments and simulation analysis for studying the hydration water dynamics of *N*-acetyl-leucine-methylamide (NALMA) solutions as a function of concentration and temperature. The experiments show non-Arrhenius translational dynamics over the temperature range of −3 to +37 °C for all concentrations, and fits to the experimental intermediate scattering function show nonexponential relaxation dynamics. While the lower-concentration NALMA solution could be classified as an intermediate to strong liquid, the higher concentration is legitimately defined as a fragile liquid, and the hydration dynamics of the most concentrated solution exhibits very good correspondence with the same signatures of non-Arrhenius behavior and nonexponential dynamics as that observed for supercooled water well below −20 °C. The corresponding molecular dynamics simulation analysis of the high concentration data using the SPC water model, a common companion water model used in protein simulations, is severely limited in application to the dynamics of this system because of the very low temperature of maximum density of the SPC water model. However, the simulations are informative in the sense that nonexponential relaxation is still evident at the effectively higher temperatures, which indicates that the underlying potential energy surface is very rough at high concentrations, although the sampling is still sufficiently ergodic so that Arrhenius behavior is observed. We provide discussion in regards to the mutually beneficial connection between supercooled liquids and glasses and its biological importance for protein−water systems.

Introduction

The observation that water dynamics near protein surfaces shows nonexponential thermal relaxation processes[1] has led to active exploration in two intimately related areas: whether protein−water systems bear sufficient analogy and, therefore, are informative about the nature of glass formers[2,3] and what the biological implications are if such a relationship existed between the two systems.[1,4] Our own exploration of the area has focused on understanding the hydration environment of proteins through the study of individual blocked amino acids as a function of their concentration in water.[4−7] This invokes the zeroth-order concept that polymers can be modeled by increasing the effective local concentration of monomers, giving rise to a situation resembling a much denser liquid of monomers in the local vicinity of the chain as it collapses, which defines a model experimental system that can address the role of water in the folding of proteins[6] or hydration dynamics and protein function.[4]

In previous work we focused on the structural organization of dilute to very high concentration solutions of a prototypical hydrophobic amino acid, *N*-acetyl-leucine-methylamide (NALMA), using neutron[7] and X-ray scattering experiments[5] and molecular dynamics (MD) simulations.[6] Those combined studies found that, throughout the full concentration range of 0.5−2.0 M studied, water stabilizes monodispersed and small clusters of amino acids, as opposed to more complete segregation of the hydrophobic monomers into a sequestered core. These results are consistent with a requirement of overcoming a desolvation barrier to reach the native state. In fact this is a mechanism that has been observed in a number of MD protein folding simulations, including the refolding of a beta-hairpin fragment of protein G[8] and all-atom folding simulations of protein G and src-SH3.[9−11]

Recently we have turned to the study of the hydration dynamics of the NALMA−water system as a function of concentration.[4] We reported quasi-elastic neutron scattering (QENS) experiments and accompanying interpretation and analysis using MD, to probe the evolution of water dynamics at room temperature from dilute to very high concentration solutions of NALMA in water, for both the completely deuterated and completely hydrogenated leucine monomer.[4] The NALMA−water system and the QENS data together provide a unique study for characterizing the dynamics of different hydration layers near a prototypical hydrophobic side chain and the backbone to which it is attached. The 2.0 M data are interesting in particular because we know from our structural studies that the solutions organize so that only one water layer separates NALMA solutes; that is, it unambiguously measures the dynamics of a single hydration layer directly. It is important to note that ∼50−60% of a folded protein's surface is hydrophobic,[12] which makes this choice of amino acid an important distinguishing feature of our study of protein−water dynamics and connection to glass formers compared to previous studies that studied purely hydrophilic polypeptides.[3]

* Corresponding author: e-mail tlhead-gordon@lbl.gov.
† Part of the special issue "Frank H. Stillinger Festschrift".
‡ Department of Bioengineering, University of California.
§ Both authors contributed equally to this work.
|| Graduate Group in Biophysics, University of California.
⊥ National Institute of Standards and Technology.

10.1021/jp046847p CCC: $27.50
Published on Web 11/10/2004

We observed several unexpected features in the dynamics of these biological solutions under ambient conditions. The NALMA dynamics shows evidence of de Gennes narrowing, an indication of coherent long time scale structural relaxation dynamics.[4] The translational and rotational water dynamics at the highest solute concentrations are found to be highly suppressed as characterized by long residential time and slow diffusion coefficients, corresponding to lightly supercooled water at −10 °C.[4] The analysis of the more dilute concentration solutions determined that for outer layer hydration dynamics the translational diffusion dynamics is still suppressed, although the rotational relaxation time and residential time are converged to bulk-water values. Finally, MD analysis of the first hydration shell water dynamics shows spatially heterogeneous water dynamics, as measured by residence times and orientational correlations, with fast water motions near the hydrophobic side chain and much slower water motions near the hydrophilic backbone.[4]

These tantalizing initial results on unusual hydration and solute dynamics of the room temperature solutions has led us to now considering the temperature dependence of these model biological systems to draw out more instructive information about their connection to glassy dynamics, although we emphasize that these new results are still somewhat preliminary. Over the (limited) temperature range of the experiments, we find that the 0.5 M solution shows a weakly non-Arrhenius behavior in its water translational dynamics with temperature, and the corresponding 2.0 M solutions are clearly super-Arrhenius, while the rotational dynamics are found to be Arrhenius within the larger experimental error bars for both concentrations over the same temperature range. Furthermore, the experimental intermediate scattering function, when fit to a stretched exponential, shows strong deviations from exponential dynamics that indicates that slow relaxation processes exhibiting spatial heterogeneity are present. The corresponding MD analysis qualitatively confirms some of these signatures of nonexponential relaxation processes in the solutions, although the SPC water model,[23] commonly used in conjunction with protein simulations, is much too crude to encourage us to explore much further outside the experimental temperature range, and we plan on better simulations using the recently introduced TIP4P-EW model[13] in future work. As is appropriate for this Festschrift in honor of Frank Stillinger, we provide ample speculation as to the importance of these results and what questions we anticipate following up in near-future studies, including inherent structure analysis of the underlying potential energy surface.[14,15]

Materials and Methods

Experimental Procedure. The completely deuterated *N*-acetyl-(d_3)-leucine(d_{10})-methylamide(d_3) (molecular weight 202.25) was purchased from CDN Isotopes, Canada. The solution samples were obtained by dissolution of the completely deuterated amino acid powder in pure H_2O at 2.0 M, and the 0.5 M low-concentration sample has been obtained by dilution of the 2.0 M solution. To remove small aggregates from the solution, the sample was centrifuged (10 min at 10 000*g*) before measurement.

The QENS experiment was carried out at the NIST Center for Neutron Research, using the disk chopper time-of-flight spectrometer (DCS).[16] To better separate the translational and rotational components in the spectra, two sets of experiments were performed using different incident neutron wavelengths of 7.5 and 5.5 Å to give two different energy resolutions. The DCS operating at $\lambda = 7.5$ Å with an incident energy of $E_{inc} = 1.45$ meV gives a wave vector range of $0.15 < Q < 1.57$ Å^{-1} and an energy resolution of 35 μeV at full width at half-maximum (FWHM). At $\lambda = 5.5$ Å and $E_{inc} = 2.7$ meV, the wave vector range covers $0.20 < Q < 2.15$ Å^{-1} with a FWHM of 81 μeV.

The sample containers were two concentric cylinders with radii differing by 0.1 mm. The data collection lasted for about 8−12 h per sample, depending on the resolution, to facilitate statistical analysis. All spectra were corrected for the contribution made by the sample holder. Detector efficiencies, energy resolution, and normalization are measured with standard vanadium. The resulting data were corrected and analyzed with DAVE programs (http://www.ncnr.nist.gov/dave/). Water dynamics measurements were performed at −3, 4, and 37 °C for the 2 M solution and 4 and 37 °C for the 0.5 M solution. We analyze these new temperature points with previous QENS measurements for both concentrations at 27 °C.[4]

Experimental Analysis. The quasi-elastic neutron experiment measures the incoherent differential cross section:

$$\frac{d^2\sigma}{dE\, d\Omega} = \frac{\sigma_{inc}}{4\pi}\frac{k_s}{k_i} N S_{inc}(Q, \omega) \tag{1}$$

where σ_{inc} is the total incoherent cross section, k_i and k_s are the wavevector of the incident and scattered neutron, Q is the momentum transfer, ω is the frequency, and $S_{inc}(Q, \omega)$ is the incoherent dynamic structure factor. The analysis of the resulting spectra relies on a fit to the incoherent dynamic structure factor with several Lorentzian contributions convoluted with the instrumental resolution. On the basis of those fits we were able to further interpret the data using the following analytical models traditionally applied to liquids.[18,19]

The first assumption is that $S_{inc}(Q, \omega)$ can be expressed as a convolution of three different kinds of proton motion:[18,19]

$$S_{inc}(Q, \omega) = e^{-1/3Q^2\langle u^2\rangle} S_{inc}^{trans}(Q, \omega) \otimes S_{inc}^{rot}(Q, \omega) \tag{2}$$

where the exponential term is the Debye Waller factor, which represents the vibration in the quasi-elastic region; the $\langle u^2\rangle$ term is the mean square displacement. The second and third terms are the translational and rotational incoherent dynamic structure factors, respectively. The scattering law for translation is described as

$$S_{inc}^{trans}(Q, \omega) = \frac{1}{\pi}\frac{\Gamma_{trans}(Q)}{\omega^2 + [\Gamma_{trans}(Q)]^2} \tag{3}$$

where Γ_{trans} is the half width at half-maximum of a Lorentzian function. We have found that the Lorentzian for translation is best fit to a random jump diffusion model, which considers the residence time τ_0 for one site in a given network before jumping to another site[20]

$$\Gamma_{trans}^{J}(Q) = \frac{D_{trans}Q^2}{1 + D_{trans}Q^2\tau_0} \tag{4}$$

where the mean jump diffusion length L is defined in this model as $L = (6D_{trans}\tau_0)^{1/2}$ and D_{trans} is the translational diffusion coefficient.

Water rotational relaxation has been described using the diffusion model for hindered rotation on the surface of a sphere.[21] The rotational incoherent dynamic structure factor is

$$S_{\mathrm{inc}}^{\mathrm{rot}}(Q,\omega) = j_0^{\,2}(Qa)\,\delta(\omega) + \sum_{l=1}(2l+1)\,j_l^{\,2}(Qa)\,\frac{1}{\pi}\,\frac{l(l+1)D_{\mathrm{rot}}}{\omega^2 + [l(l+1)D_{\mathrm{rot}}]^2} \quad (5)$$

where $j_l(Q)$ is a spherical Bessel function of order l; a is the radius of the sphere; and D_{rot} is the rotational diffusion coefficient. For $l = 1$, which dominates the second term of eq 5, the half width at half-maximum is $\Gamma_{\mathrm{rot}} = 2D_{\mathrm{rot}}$, which corresponds to a rotational characteristic time of $\tau_{\mathrm{rotation}} = 1/6D_{\mathrm{rot}}$.

Theoretical Analysis. We used MD to simulate the same experimental observables evaluated by the QENS experiments for aqueous NALMA solutions at 2.0 M. The assisted model building with energy refinement (AMBER) force field due to Cornell et al.[22] and the SPC water model[23] were used for modeling the NALMA solute and water, respectively. Five separate MD simulations were carried out at −10, −5, 4, 25, and 37 °C in the NVT ensemble using velocity Verlet integration and velocity rescaling, with a time step of 1.0 fs. Ewald sums were used for calculation of the long-range Coulomb forces. Rigid-body dynamics for the water solvent were integrated using RATTLE.[24] For the analysis of the water dynamics in the NALMA aqueous solutions, we performed simulations of a dispersed solute configuration consistent with our structural analysis.[6] At temperatures of 37, 25, and 4 °C, the simulations were equilibrated for 0.2 ns and statistics were gathered over 1.0 ns. For the −5 °C simulation we equilibrated for 0.3 ns and collected statistics for 1.2 ns, and for −10 °C we equilibrated for 0.4 ns and collected statistics for 1.3 ns.

We used the Einstein relation to derive the translational self-diffusion coefficients from the mean square displacement of water oxygens, and the rotational dynamics using the orientational autocorrelation function:

$$P_2(t) = \langle 0.5[3\cos^2\theta(t) - 1]\rangle \quad (6)$$

where $\theta(t)$ measures the angle between the dipole vector of the water molecule at times t and 0 and the angle brackets denote an ensemble average at a given temperature. We also evaluated the self-intermediate scattering factor for hydrogens:

$$F_{\mathrm{H}}^{\mathrm{S}}(Q,t) = \frac{1}{N}\langle \exp[+i\mathbf{Q}\cdot\mathbf{R}_{\mathbf{H}}(0)]\,\exp[-i\mathbf{Q}\cdot\mathbf{R}_{\mathbf{H}}(t)]\rangle \quad (7)$$

where the angular brackets denote an ensemble average at a given temperature and $\mathbf{R}_{\mathbf{H}}(t)$ denotes the position of a given water hydrogen at time t.

Experimental Results

Hydration Water Dynamics. The scattering profile of the completely deuterated solute in H_2O has been measured to characterize the hydration water dynamics at various concentrations and temperatures. The higher resolution experiment primarily measures the slow translational dynamics, while the lower resolution experiment contains information about both rotational and translational water proton motion. The experiments done at two different resolutions, in principle, permit us to separately resolve the proton motion time scales for translation and rotation and are discussed separately. We return to the validity of this assumption later.

As we have already reported for the room-temperature data,[4] the fit to the data generated at high resolution for −3, 4, and 37 °C, which probes the slower components of hydration dynamics, all required two Lorentzians and a flat background. The fit has been performed between ±0.9 meV, and the background component takes into account all movements that are too fast to be detected at the defined resolution, such as low energy vibrational modes. Figure 1 shows the fitted incoherent scattering function for the 2 M data at 4 °C at $Q \sim 1.25$ Å^{-1}, which is typical of the quality of fit we obtained in the experimental analysis. There is a broad Lorentzian which describes faster movements that are tentatively identified as rotational and, thus, will be analyzed simultaneously with the low-resolution data. The narrow Lorentzian function is indicative of translational motion, and on the basis of the dependence of $\Gamma(Q)$ with Q^2, is best described with a jump diffusion model.

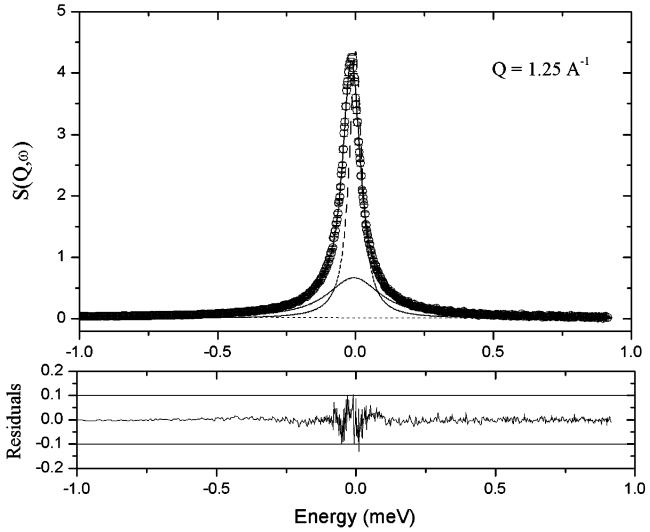

Figure 1. Incoherent structure factor spectrum for 2.0 M NALMA concentration in H_2O, at 4 °C, measured at 35 μeV at $Q \sim 1.25$ Å^{-1} (open symbols). The solid line is the total fit component resulting from the convolution of the two Lorentzian functions and the flat background. The Lorentzian fits to the spectra (dashed lines) show good separation of widths and intensities and are typical of the quality of fit for all spectra measured in this study. The residuals show that the quality of fit is good in the energy range of the experiment.

TABLE 1: Experimental Values for Water Dynamics for 0.5 M NALMA as a Function of Temperature

	temperature		
	4 °C	25 °C	37 °C
D_{trans} (10^{-5} cm^2/s; JD[a])	0.9	1.65	2.0
τ_0 (ps; JD[a])	1.8	0.94	0.7
D_{trans} (10^{-5} cm^2/s; ISF[b])	0.71	1.25	1.79
τ_{rotation} (ps; HR[c])	1.68	1.0	0.9

[a] Translational diffusion coefficient, D_{trans}, and the residence time, τ_0, of water based on the jump diffusion model. [b] Translational diffusion coefficient, D_{trans}, based on the analysis from the experimental intermediate scattering function. [c] Rotational time scale for water, τ_{rotation}, based on the Sears hindered rotation model.

The resulting diffusion coefficient, D_{trans}, and residential time τ_0 obtained at 2 M and 0.5 M concentrations as a function of temperature are shown in Tables 1 and 2. Figure 2 plots the temperature dependence of the translational diffusion coefficient for pure liquid water,[25] and the hydration water for the 0.5 and 2.0 M NALMA solutions. It is especially evident from the plot that the 2.0 M data has a diffusion coefficient at −3 °C that looks like that of supercooled water below −20 °C.

Figure 3 displays an Arrhenius plot of the translational diffusion coefficient of hydration water for both concentrations; the 0.5 M NALMA concentration is weakly non-Arrhenius over the temperature range of 4−37 °C, while the 2.0 M data is super-

TABLE 2: Experimental and Simulation (in Parentheses) Values for Water Dynamics for 2.0 M NALMA as a Function of Temperature

	temperature			
	−3 °C (−5 °C)	4 °C	25 °C	37 °C
D_{trans} (10^{-5} cm^2/s; JD[a])	0.22(1.2)	0.35(1.5)	0.75(2.2)	0.85(2.92)
τ_0 (ps; JD[a])	7.33	6.9	3.6	2.5
D_{trans} (10^{-5} cm^2/s; ISF[b])	0.19	0.28	0.67	0.75
$\tau_{rotation}$ (ps; HR[c])	2.7(4.4)	2.5	2.2(2.4)	1.9(1.8)

[a] Translational diffusion coefficient, D_{trans}, and the residence time, τ_0, of water based on the jump diffusion model. [b] Translational diffusion coefficient, D_{trans}, based on the analysis from the experimental intermediate scattering function. [c] Rotational time scale for water, $\tau_{rotation}$, based on the Sears hindered rotation model.

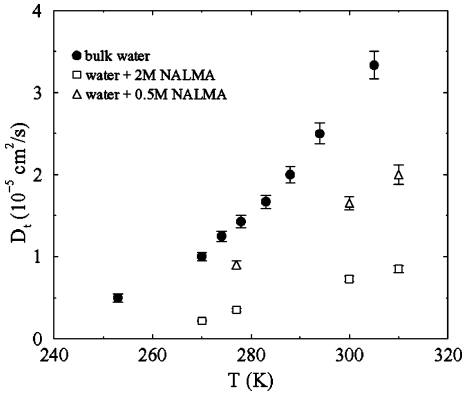

Figure 2. Values of the translational diffusion coefficient as a function of temperature from QENS experiments and fits based on the jump diffusion model for pure liquid water reported in ref 23 and as measured here for 2 and 0.5 M NALMA solutions. The water diffusion coefficient for the NALMA solutions shows a non-negligible suppression when compared to the bulk water results at the same temperature value.

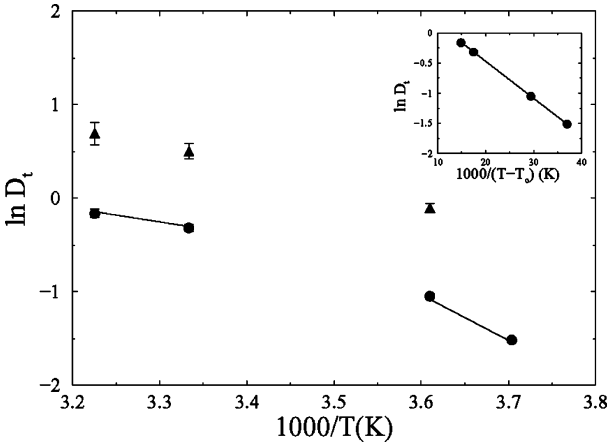

Figure 3. Arrhenius representation for the translational diffusion coefficient for 2 and 0.5 M NALMA concentrations from experiment. The inset shows the fit to the VFT equation for the 2 M diffusion coefficient data. The critical temperature for the diffusion T_0 is ∼245 K.

Arrhenius (strong curvature of the logarithmic plots versus inverse temperature)[26,27] over the same temperature range. The additional QENS experiment at −3 °C for the higher concentration confirms the super-Arrhenius character of the 2 M water translational diffusion data, suggesting that the molecular mechanism of the hydration dynamics changes abruptly between 25 and 4 °C for the high NALMA concentration solution, with activation barriers of ∼3.0 and ∼10.0 kcal/mol above and below the transition temperature, respectively. The super-Arrhenius

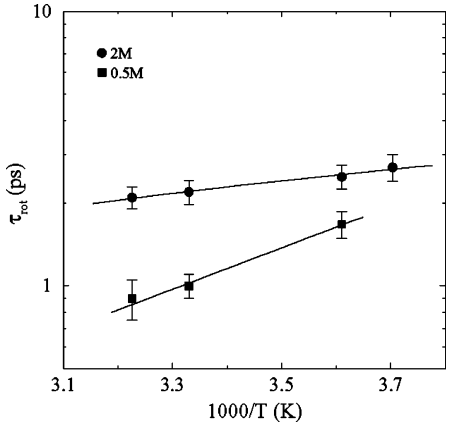

Figure 4. Arrhenius representation for the rotational relaxation time for 2 and 0.5 M NALMA concentration from experiment. The straight lines are the best fit to the Arrhenius expression in the investigated temperature range, which gives activation energy values of ∼3.0 and ∼1.5 kcal/mol for the low and high concentrations, respectively.

dependence of the diffusion dynamics at 2 M is well-supported by the small experimental error bars and would not change with more temperature points. In regard to the 0.5 M data, the only question is whether the dynamics will change from non-Arrhenius to super-Arrhenius over a larger temperature range.

In the inset of the same figure we replot the 2.0 M hydration water diffusion data and its deviation from Arrhenius behavior using the Vogel−Fulcher−Tammann (VFT) equation

$$D_t = A \exp\left[-\frac{B}{(T - T_0)}\right] \tag{8}$$

where A, B, and T_0 are three parameters with some physical meaning in regard to true glass formers.[2,26] Similar to what has been observed for other fragile glass formers, the fit to the VFT equation is excellent.

The data from the low-resolution runs, probing water rotational motion, were analyzed by including the narrow translational Lorentzian functions based on the high-resolution experiment as known values and using eq 5. The best fit, performed between ±2 meV, has been obtained by including two additional free Lorentzian functions ($l = 1, 2$ of eq 5) and a flat background. The resulting $\tau_{rotation}$ as a function of temperature and concentration is given in Tables 1 and 2. When plotted in an Arrhenius representation, the 0.5 and the 2 M rotational data show a normal Arrhenius temperature dependence (Figure 4). Given the limited temperature range of the experimental data, a greater temperature range to confirm the Arrhenius behavior is clearly required.

For bulk water and water in NALMA solutions, the fast component of the rotational dynamics corresponds to librational motion that can be related to the average hydrogen bond lifetime,[25,28] while the residential time of the jump diffusion model is a direct measure of the time duration that is necessary for a water molecule to break from its hydrogen-bonded neighbors by rotational excitation.[25,28] At high temperature, when most water molecules have weakened hydrogen bonds, the residential time is largely equivalent to the time scale of librational motion of the hydrogen-bond dynamics. At lower temperatures (or higher NALMA concentrations) the time scales for local librational motion are shorter than the measured residence time scales because waters are caged by local neighbors, requiring a cooperative motion to execute diffusion. This caging effect is crudely captured by the jump diffusion

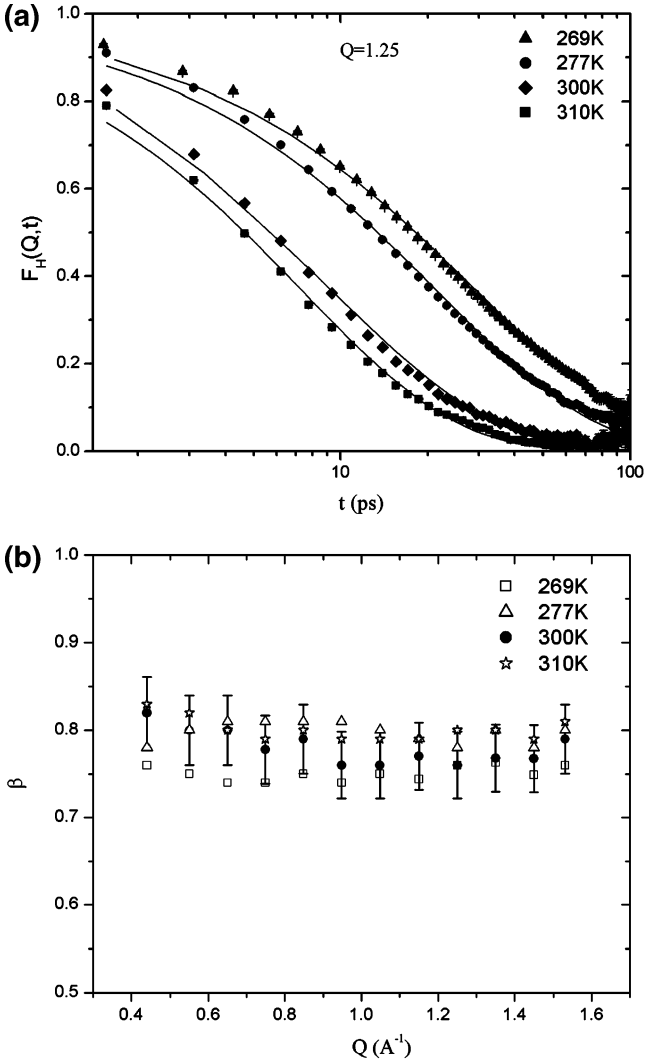

Figure 5. (a) Self-intermediate scattering function from experiment. For the 2 M solution at $Q = 1.25$ Å^{-1} as a function of temperature (symbols), along with the stretched exponential fit (line). (b) The Q dependence of the stretched exponential parameter β from the fit to the experimental intermediate scattering function in (a) as a function of temperature. We show the error bar in regard to the fit for the room-temperature data only, and similar error bars were found for the other temperatures as well.

model through its average residence time scale parameter τ_0 that represents deviations from normal Brownian diffusion.

To consider a complementary analysis of the NALMA system, we analyze the experimental intermediate scattering function for hydrogens, $F_H(Q, t)$, at 2.0 M. The intermediate scattering function has been generated using the fast Fourier transform option in the DAVE package; to avoid contribution of the fast dynamics component (previously characterized as librational/rotational movement) we subtracted out the first 5 ps of data and renormalized $F_H(Q, t)$ at the new time origin to unity. The Fourier transformed $S(Q, \omega)$ for all four temperatures at $Q \sim 1.25$ Å^{-1} using the higher resolution QENS data is shown in Figure 5a.

We then fit the long-time decay of $F_H(Q, t)$ to a stretched exponential form

$$F_H(Q, t) = \exp[-(t/\tau)^{\beta}] \qquad (9)$$

where deviations from $\beta = 1$ is a signature of a pronounced slow down in dynamical processes with a characteristic relaxation time τ, which is believed to be related to spatial heterogeneity in the dynamics.[26,29,30] In fact, the origin of the nonexponential form is the reflection of anomalous diffusion which is controlled by a local structural relaxation or "cage effect" as described in mode coupling theory applied to supercooled liquids.[30−32] The dependence of $1/\tau$ versus Q^2 is then proportional to the water diffusion coefficient in the limit of $Q \rightarrow 0$ and numerically evaluated from the slope for $Q <$ 1.0 Å^{-1}. As shown in Tables 1 and 2, we find good agreement between the diffusion coefficient inferred from the stretched exponential analysis and that from the jump diffusion model.

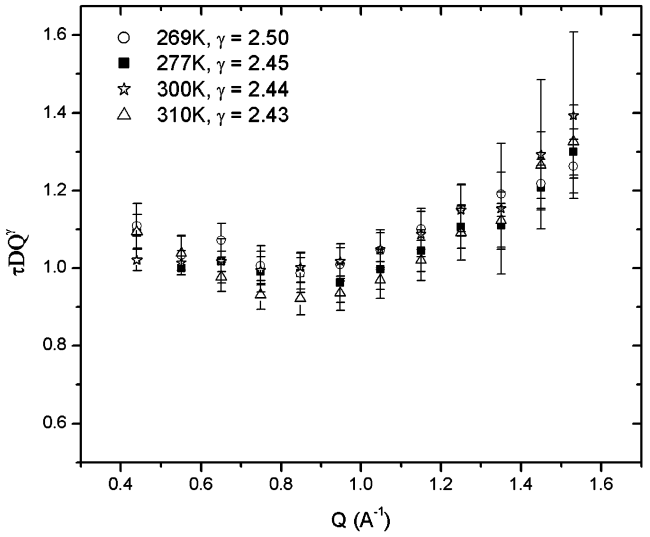

Figure 6. Plot of $\tau D_{trans} Q^{\gamma}$ versus Q as a function of temperature for hydration dynamics for 2 M NALMA from the QENS experiment and stretched exponential fits to the intermediate scattering function. We note that strictly $\gamma = 2$ so that $\tau D_{trans} Q^2 = 1$ for $Q \rightarrow 0$ are descriptions of normal diffusion. Given the finite range of Q data (smallest $Q \sim$ 0.4 Å^{-1}) from experiment, as well as experimental error, this is only approximated with $\gamma \sim 2.5$ at the smallest Q values measured. Given that caveat, we measure positive deviations from 1 at high Q values for all the temperatures investigated and a corresponding decrease of γ to ∼1.8.

Figure 5b reports the Q dependence of the fitted β-value exponents as a function of temperature for 2.0 M. The qualitative behavior of the temperature dependence of the exponent β is relatively flat (as also seen in refs 33 and 34) but deviates significantly from 1, reaching values as low as 0.75 for the lowest temperature studied. This further confirms the underlying anomalous diffusion behavior that signals the fragility of the water liquid in high concentration NALMA solutions.

In Figure 6 we plot $\tau D_{trans} Q^{\gamma}$ versus Q as a function of temperature, where τ is the relaxation time as defined in eq 9, D_{trans} is the diffusion coefficient as extrapolated from $1/\tau$ versus Q^2, and γ is a fitting parameter given the uncertainty in the experimental data. We note that strictly $\gamma = 2$ so that $\tau D_{trans} Q^2 = 1$ for $Q \rightarrow 0$ are descriptions of normal diffusion. Given the finite range of Q data (smallest $Q \sim 0.4$ Å^{-1}) from experiment, this is only approximated with $\gamma \sim 2.5$ at the smallest Q values measured. Given the caveat of finite Q data, we measure deviations from 1 at high Q values for all the temperatures investigated. We further observe that τ follows a power law in Q, $1/\tau \propto Q^{\gamma}$, where the exponent γ decreases gradually to ∼1.8 for $Q >$ 1.0 Å^{-1}, similar to what has been observed earlier from MD simulations in supercooled water.[35] The strong curvature as shown in Figure 6 suggests the presence of an anomalous diffusion process over small length scales, which in supercooled water has been attributed to the structural

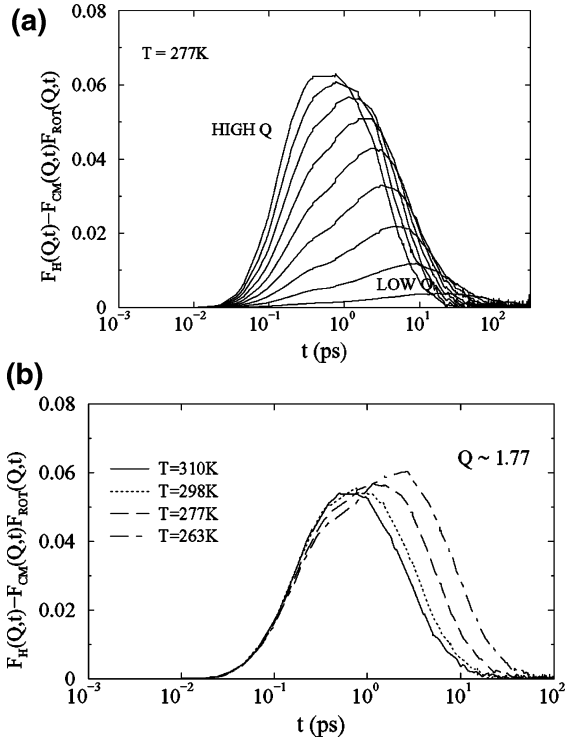

Figure 7. (a) Semilogarithmic plot of the connected intermediate scattering function, for the 2 M solution, $F_{CON}(Q, t)$ versus t for hydrogen atoms as a function of Q. For nine integer multiples of $Q = 0.253$ Å^{-1}, the correlation function grows with Q. (b) Semilogarithmic plot of the connected intermediate scattering function, for the 2 M solution, $F_{CON}(Q, t)$ versus t for hydrogen atoms as a function of temperature, for $Q = 1.77$ Å^{-1}.

relaxation of the cage of surrounding molecules that represent a stable potential energy minimum surrounded by high barriers.[31]

Theoretical Results

Hydration Water Dynamics. We have performed MD simulations for the NALMA solutions over the same limited temperature range of the experiment for the 2.0 M solution, to confirm that the trends in dynamic signatures exhibited by experiment are matched by the theoretical results. We have performed additional simulations at −10 °C to better characterize the dynamical signatures of this glassy system.

The simulated $F_H(Q, t)$ can be used to estimate errors in the assumption of a decoupling of translational and rotational motions. In Figure 7a,b we plot the connected intermediate scattering function, $F_{CON}(Q, t)$

$$F_{CON}(Q, t) = F_H(Q, t) - F_{CM}(Q, t)\, F_{ROT}(Q, t)$$

as a function of Q and temperature, respectively. It is clear that overall the decoupling approximation gives acceptable error, except for Q vectors corresponding to near the maximum in the scattering intensity where errors reach as high as 6−7%, only slightly smaller than reported in ref 35 on pure supercooled water.

In Table 2 we report the simulated translational diffusion constant and the rotational time scale τ_{rot} [obtained from the stretched exponential fit to $P_2(t)$] and present their temperature dependence in Figure 8a,b. The SPC model shows spectacular failure in exhibiting the requisite non-Arrhenius behavior of the translational water motion, and by association the rotational motion must be suspect as well. This is not surprising given the fact that the temperature of maximum (TMD) density for SPC water is −31 °C, so that the effective simulated temperature

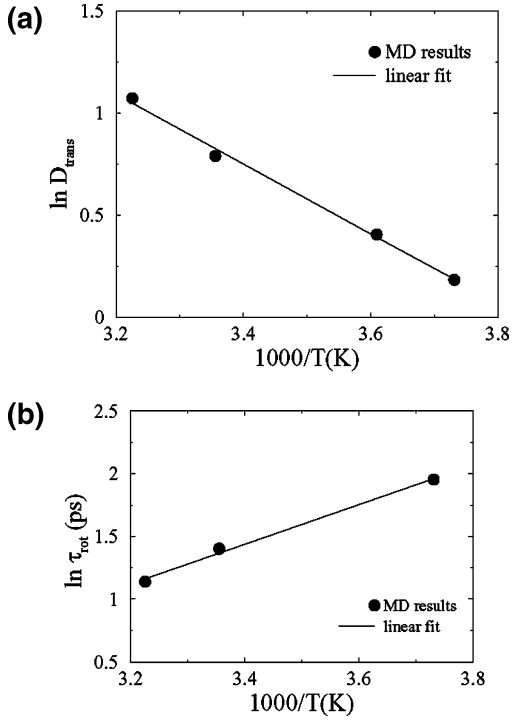

Figure 8. (a) Arrhenius plot of the translational diffusion coefficient from MD simulation for the 2 M solution. The solid line is a linear fit to the simulation data, which is in conflict with experiment. (b) Arrhenius plot of the rotation relaxation time obtained from the stretched exponential fit to $P_2(t)$ for the 2 M solution. The solid line is again a linear fit to the simulation data.

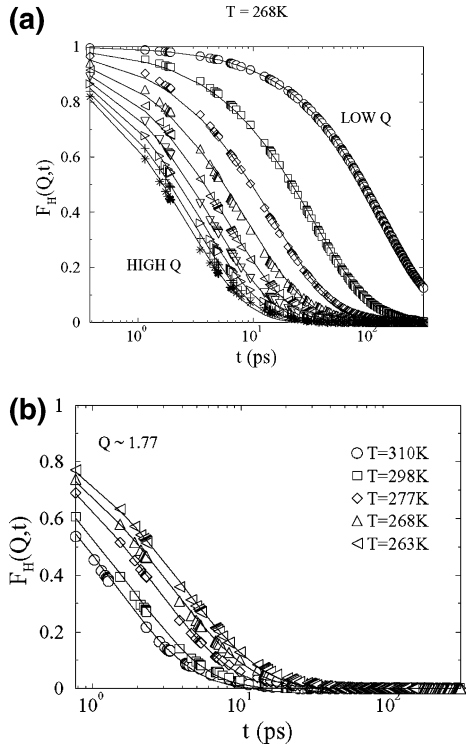

Figure 9. Self-intermediate scattering function, calculated from MD simulation. (a) For the 2 M solution at $T = 268$ K as a function of Q (symbols), along with the stretched exponential fit (line). (b) For the 2 M solution at $Q = 1.77$ Å^{-1} as a function of temperature (symbols), along with the stretched exponential fit (line).

is much higher than that probed in the QENS experiments. While it is commonly assumed that protein force fields are best used with the simple water models, like SPC, against which

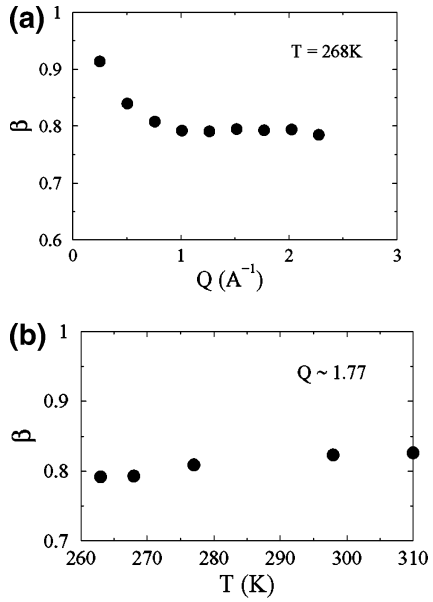

Figure 10. Stretched exponential parameter β (a) as a function of Q and (b) as a function of temperature.

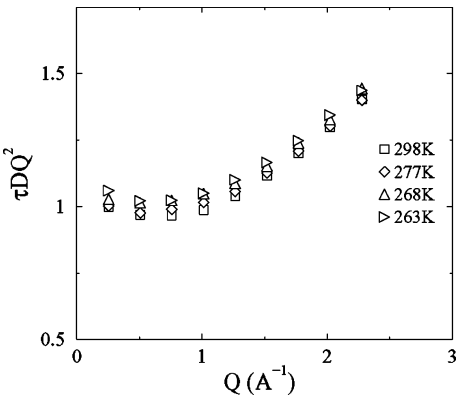

Figure 11. Plot of simulated $\tau D_{trans}Q^2$ versus Q as a function of temperature. The behavior is similar to that observed experimentally in Figure 6 and as reported in other simulations of bulk supercooled water.

they are parametrized, it is clear that their continued application in protein water simulations is counterproductive, especially for the study of dynamics.

Figure 9a,b plots the simulated $F_H(Q, t)$ as a function of Q (at 268 K) and temperature (for $Q = 1.77$ Å^{-1}, near the maximum of the O−O static structure factor), respectively. Evidence of slow relaxation is evident in the simulated $F_H(Q, t)$, when we fit it to a stretched exponential form using eq 9. The same pronounced slow down in relaxation processes, characterized by the exponent β, shows both a clear Q dependence (Figure 10a) and temperature dependence (Figure 10b).

In Figure 11 we plot $\tau D_{trans}Q^2$ versus Q as a function of temperature, where τ is the relaxation time as defined in eq 9. We observe that $\tau D_{trans}Q^2 = 1$ at low Q values, while significant deviations from 1 are present at high Q values for all the temperatures investigated. The observed deviation is in agreement with the experimental translational diffusion data results which show a deviation from the hydrodynamics regime at high Q values. Simulation also gives a power law behavior in Q, $1/\tau \propto Q^{\gamma}$, where the exponent γ is 2 for systems executing normal diffusion[31,36,37] but which decreases gradually to 1.5 for $Q > 1.0$ Å^{-1}, similar to that observed experimentally in Figure 6.

Discussion and Conclusion

In this paper we have presented new QENS experiments and simulation analysis for studying the hydration water dynamics in hydrophobic amino acid monomer solutions as a function of concentration and temperature. We have found from experiment a non-Arrhenius water translational dynamics over the temperature range of −3 to 37 °C and related slow relaxation processes that are clearly nonexponential. The experimental incoherent structure factor data and its Fourier transform, the intermediate scattering function, were analyzed with a jump diffusion model and stretched exponential fits, respectively, and provided a satisfying self-consistency of the derived translational diffusion coefficients using the different data analysis procedures. While the lower concentration solution could be classified as an intermediate to strong liquid, the 2.0 M concentration is legitimately defined as a fragile liquid. In fact the hydration dynamics of these solutions over the limited temperature range studied exhibit very good correspondence with the same signatures of glassy behavior, non-Arrhenius behavior, and nonexponential kinetics as that observed for supercooled water below −20 °C.[25]

The corresponding MD simulation analysis of the 2.0 M data using the SPC water model, a common companion water model used in protein simulations, is severely limited in application to the dynamics of this system because the effective simulation temperature is much higher than that of the experiment because the TMD of the SPC model is −31 °C. However, the simulations are informative in the sense that nonexponential relaxation is still evident at the effectively higher temperatures, which indicates that the underlying potential energy surface is very rough at high concentration, although the sampling is still sufficiently ergodic so that Arrhenius behavior is observed. In regards to better quantitative agreement with experiment, more careful simulations using the SPC model that are performed at the correct density at 1 atm pressure would be desired, although we suspect that the non-Arrhenius dynamics seen by experiment would still not be reproduced after correction for the density.

Instead, we believe that a better water model that performs well on neat water properties over a range of temperatures and pressures is a better choice over poor water models that are more explicitly parametrized with existing protein force fields. We have recently contributed to the testing of a re-parametrization of the standard TIP4P water model for use with Ewald techniques.[13] The new model provides an overall global improvement in water properties relative to several popular nonpolarizable and polarizable water potentials, with a density maximum at approximately 1 °C, which reproduces experimental bulk densities and the enthalpy of vaporization, ΔH_{vap}, from −37.5 to 127 °C at 1 atm with an absolute average error of less than 1%.[13] Structural properties are in very good agreement with X-ray scattering experiments at temperatures between 0 and 77 °C[38] and dynamical properties such as the self-diffusion coefficient are in excellent agreement with experiment. In near-future work we will use the new TIP4P-EW water model in conjunction with the standard AMBER94 protein force field to pursue better quantitative agreement with QENS experiments on these protein solutions. Should that comparison come out favorably, we will also perform inherent structure analysis[14,15,39−41] with these improved force fields to relate the glassy dynamics we observe experimentally to features of the underlying potential-energy landscape.

What have we learned about biological function in regards to finding analogy in the dynamics with supercooled liquids and glasses? The measured dynamics allow us to propose two

hypotheses concerning protein function. The first stems from the observation that until a critical hydration level is reached proteins do not function, and it is believed that this has to do with the dynamics of protein surface water,[42−44] although the molecular mechanism is unknown. Below the critical hydration level, as measured by 2.0 M water dynamics, we find that the water translational and rotational dynamics are very slow. Some hydration waters are tightly bound to the surface, especially near hydrophilic regions, and their slow dynamics suggest a large barrier to rearrangement with other waters. At sufficiently high levels of hydration, as measured by the 0.5 M dynamics, we find that the inner sphere water translational and rotational dynamics are still slow (equivalent to 2.0 M) but that the barrier to exchange with outer sphere waters is apparently lower, with diffusion time scales between inner and outer sphere regions approaching more bulk-like values. Therefore, we might view the catalyzing effect of "sufficient" water on side chain rearrangement on the protein surface (that is necessary for protein folding or function) as arising from a second hydration layer that lowers the barriers for water solvent rearrangement, that is, restoration of the plasticity of the water network itself.

The second hypothesis concerns transport properties of small molecules and metabolites into protein active sites. As a result of the high density of molecules within the cell, there can on average only be two to three hydration layers between proteins.[45] Because we see spatially heterogeneous dynamics at all hydration levels we have examined, that is, water motions near the hydrophobic side chain that are ∼10 times faster than water motions near the hydrophilic backbone, we propose that the difference in water time scales near hydrophobic versus hydrophilic regions might have functional importance in the crowded cell or at a protein−protein interface. We would hypothesize that hydrophilic and hydrophobic patterns on protein surfaces should be analyzed for "water slip streams" into active sites, with our results suggesting that one follow fast hydrophobic tributaries, or for protein−protein molecular recognition events involving arrested water motions to aid docking.[4] It would seem that water on this planet has played a highly influential, but still largely hidden, role of exerting evolutionary pressure to adapt amino acid sequences (and, therefore, protein folds) to exploit its many anomalies for enhanced biological function, a possibility that merits further and deeper investigation. Therefore, the study of supercooled water and glass former dynamics has an undeniably important connection to biological function in our view.

What have we learned about the dynamics of glass formers or supercooled liquids by studying these model biological systems as a function of concentration and temperature? We have learned with some reasonable certainty that the hydration dynamics measured for a solution of highly concentrated NALMA looks analogous to hydration dynamics measured for the bulk deeply supercooled liquid, in particular for the nonexponential relaxation metric of β which shows similar trends with Q and temperature. Spatial heterogeneity in the water dynamics in the two regions of the peptide is clearly evident in our simulations[4] and those reported elsewhere,[48] and numerous studies have reported on the distinct water structure features near hydrophobic and hydrophilic groups. It is important to note that, when water is presented with a purely hydrophobic or hydrophilic solute of the same size, its dynamical time scales are not that different in the two cases.[46,47] It is the heterogeneity of the chemistry (hydrophobic side chain and hydrophilic backbone) that enforces the heterogeneity in the water dynamics.

We might, therefore, speculate that the NALMA solutes provide a template or description of different structural domains with different dynamics that might exist in the bulk supercooled liquid. In particular, the NALMA solutes set up a spatially heterogeneous environment for its interactions with water, one area that permits long-lived hydrogen bonding with the peptide backbone that nucleates and stabilizes one type of water-hydrogen-bonded network, while a different, and dynamically less long-lived water-hydrogen-bonded water network arises because of no direct hydrogen-bonding interactions with the hydrophobic side chain. While the water-hydrogen-bonded networks in these domains are dynamically and structurally distinct, they are nonetheless incommensurate with each other so that their close proximity (based on the high concentration and structural organization of these solutions) would introduce an anomaly in the water diffusion at the interface of these domains, requiring a coordinated motion of a number of water molecules to negotiate a mutually agreeable water network interface between them. More work needs to be completed to confirm the usefulness of such a hypothesis but provides the type of speculative structural connections between water ordering near hydrophobic groups and dynamical processes occurring in the supercooled water state that were initially inspired by Stillinger in ref 17.

Acknowledgment. We gratefully acknowledge the support of NIH GM65239-01, and R.K.M. thanks support under NIH GM. This work utilized facilities supported in part by the National Science Foundation under Agreement No. DMR-0086210. Certain commercial materials are identified in this paper to foster understanding. Such identification does not imply recommendation or endorsement by NIST, nor does it imply that the materials or equipment identified are necessarily the best available for the purpose. D.R. thanks Jose Teixeira for constructive discussions. T.H.-G. sincerely acknowledges Frank Stillinger for his mentorship when she was at Bell Labs and the strong influence he exerts on the work described here.

References and Notes

(1) Bizzarri, A. R.; Cannistraro, S. *J. Phys. Chem. B* **2002**, *106*, 6617.
(2) Angell, C. A. *Science* **1995**, *267*, 1924.
(3) Green, J. L.; Fan, J.; Angell, C. A. *J. Phys. Chem.* **1994**, *98*, 13780.
(4) Russo, D.; Hura, G.; Head-Gordon, T. *Biophys. J.* **2004**, *86*, 1852.
(5) Hura, G.; Sorenson, J. M.; Glaeser, R. M.; Head-Gordon, T. *Perspect. Drug Discovery Des.* **1999**, *17*, 97.
(6) Sorenson, J. M.; Hura, G.; Soper, A. K.; Pertsemlidis, A.; Head-Gordon, T. *J. Phys. Chem. B* **1999**, *103*, 5413.
(7) Pertsemlidis, A.; Soper, A. K.; Sorenson, J. M.; Head-Gordon, T. *Proc. Natl. Acad. Sci. U.S.A.* **1999**, *96*, 481.
(8) Pande, V. S.; Rokhsar, D. S. *Proc. Natl. Acad. Sci. U.S.A.* **1999**, *96*, 9062.
(9) Sheinerman, F. B.; Brooks, C. L. *Proc. Natl. Acad. Sci. U.S.A.* **1998**, *95*, 1562.
(10) Shea, J. E.; Onuchic, J. N.; Brooks, C. L. *Proc. Natl. Acad. Sci. U.S.A.* **2002**, *99*, 16064.
(11) Cheung, M. S.; Garcia, A. E.; Onuchic, J. N. *Proc. Natl. Acad. Sci. U.S.A.* **2002**, *99*, 685.
(12) Janin, J. *Structure with Folding & Design* **1999**, *7*, R277.
(13) Horn, H. W.; Swope, W. C.; Pitera, J. W.; Madura, J. D.; Dick, T. J.; Hura, G. L.; Head-Gordon, T. *J. J. Chem. Phys.* **2004**.
(14) Stillinger, F. H.; Weber, T. A. *Phys. Rev. A* **1982**, *25*, 978.
(15) Stillinger, F. H.; Weber, T. A. *J. Phys. Chem.* **1983**, *87*, 2833.
(16) Copley, J. R. D.; Cook, J. C. *Chem. Phys.* **2003**, *292*, 477.
(17) Stillinger, F. H. *Science* **1980**, *209*, 451.
(18) Bee, M. *Chem. Phys.* **2003**, *292*, 121.
(19) Bee, M. *Quasi-elastic neutron scattering*; Adam Hilger: Philadelphia, 1988.
(20) Egelstaff, P. A. *An introduction to the liquid state*; Clarendon: Oxford, 1992.
(21) Sears, V. F. *Can. J. Phys.* **1966**, *44*, 1299.

(22) Cornell, W. D.; Cieplak, P.; Bayly, C. I.; Gould, I. R.; Merz, K. M.; Ferguson, D. M.; Spellmeyer, D. C.; Fox, T.; Caldwell, J. W.; Kollman, P. A. *J. Am. Chem. Soc.* **1995**, *117*, 5179.
(23) Berendsen, H. I. C.; Postma, I. P. M.; van Gunsteren, W. F.; Hermans, I. In *Intermolecular Forces*; Pullman, B., Ed.; Reidel: Dordrecht, Holland, 1981; p 31.
(24) Anderson, H. C. *J. Comput. Phys.* **1983**, *52*, 24.
(25) Teixeira, J.; Bellissentfunel, M. C.; Chen, S. H.; Dianoux, A. J. *Phys. Rev. A* **1985**, *31*, 1913.
(26) Debenedetti, P. G.; Stillinger, F. H. *Nature* **2001**, *410*, 259.
(27) Stillinger, F. H.; Debenedetti, P. G. *J. Chem. Phys.* **2002**, *116*, 3353.
(28) Bellissent-Funel, M. C.; Teixeira, J. *J. Mol. Struct.* **1991**, *250*, 213.
(29) Ediger, M. D. *Annu. Rev. Phys. Chem.* **2000**, *51*, 99.
(30) Ediger, M. D.; Angell, C. A.; Nagel, S. R. *J. Phys. Chem.* **1996**, *100*, 13200.
(31) Sciortino, F.; Gallo, P.; Tartaglia, P.; Chen, S. H. *Phys. Rev. E* **1996**, *54*, 6331.
(32) Gotze, W.; Sjogren, L. *Chem. Phys.* **1996**, *212*, 47.
(33) Faraone, A.; Liu, L.; Mou, C. Y.; Shih, P. C.; Copley, J. R. D.; Chen, S. H. *J. Chem. Phys.* **2003**, *119*, 3963.
(34) Bellissent-Funel, M. C. *J. Mol. Liq.* **2000**, *84*, 39.
(35) Chen, S. H.; Gallo, P.; Sciortino, F.; Tartaglia, P. *Phys. Rev. E* **1997**, *56*, 4231.
(36) Chen, S. H.; Liao, C.; Sciortino, F.; Gallo, P.; Tartaglia, P. *Phys. Rev. E* **1999**, *59*, 6708.
(37) Gallo, P.; Sciortino, F.; Tartaglia, P.; Chen, S. H. *Phys. Rev. Lett.* **1996**, *76*, 2730.
(38) Hura, G.; Russo, D.; Glaeser, R. M.; Head-Gordon, T.; Krack, M.; Parrinello, M. *Phys. Chem. Chem. Phys.* **2003**, *5*, 1981.
(39) Stillinger, F. H. *Science* **1995**, *267*, 1935.
(40) Sastry, S.; Debenedetti, P. G.; Stillinger, F. H. *Nature* **1998**, *393*, 554.
(41) Sastry, S. *Nature* **2001**, *409*, 164.
(42) Rupley, J. A.; Careri, G. *Adv. Protein Chem.* **1991**, *41*, 37.
(43) Doster, W.; Settles, M. The dynamical transition: The role of hydrogen bonds. *Hydration Processes in Biology*; Les Houches Lectures, 1998.
(44) Daniel, R. M.; Dunn, R. V.; Finney, J. L.; Smith, J. C. *Annu. Rev. Biophys. Biomol. Struct.* **2003**, *32*, 69.
(45) Mentre, P. *Cell. Mol. Biol.* **2001**, *47*, 709.
(46) Lynden-Bell, R. M.; Rasaiah, J. C.; Noworyta, J. P. *Pure Appl. Chem.* **2001**, *73*, 1721.
(47) Rasaiah, J. C.; Lynden-Bell, R. M. *Philos. Trans. R. Soc. London, Ser. A* **2001**, *359*, 1545.
(48) Beck, D. A. C.; Alonso, D. O. V.; Daggett, V. *Biophys. Chem.* **2003**, *100*, 221.